Adaptive Numerical Simulation of Machining Process Involving Chip Creation

S. Mohammadi[1], R. Adibi-Asl[2], M. Vaz Jr.[3]

[1] Assistant Professor, Dept. of Civil Engineering, University of Tehran, Tehran, IRAN
Homepage: http://web.ut.ac.ir/eng/cie/mohammadi, Email: smoham@ut.ac.ir
[2] Senior Research Assistant, Dept. of Mechanical Engineering, University of Tehran, IRAN
[3] Departamento de Enginharia Mecanica, univeridade do Estado Santa Catarina, Brazil

Keywords: Orthogonal machining, Blanking, Adaptive re-meshing, Shear-band

Abstract. Orthogonal machining is one of the most complex metal forming operations involving a diversity of physical phenomena, such as large deformation, complicated contact/friction condition, thermo-mechanical coupling and chip separation mechanisms. In this study, numerical simulation of this class of problems has been performed using advanced adaptive re-meshing procedures for inelastic problems, making it possible to capture shear band localization of realistic orthogonal machining. Blanking is another complex metal forming process which needs adaptive re-meshing procedure to avoid large finite element distortion. Both orthogonal machining and blanking have been numerically simulated and discussed.

Introduction

Numerical simulation of metal forming problem presents higher complexity compared to its elastic structural counterparts. Large plastic deformations not only bring complications from the mathematical point of view, but can also cause rapid solution degradation due to element distortion. Therefore, application of adaptive re-meshing techniques to this class of problems seems essential as emphasized and employed by many researchers [1-3] to simulate shear-band phenomena in machining titanium alloy.

In machining processes chips are generally classified as continuous, discontinuous (shear-band), continuous with built-up edge and shear plane oscillations [4]. The chip separation mechanisms have not been fully explained and several factors are said to affect the process whose mechanism is frequently described through plastic shear strain, shear stress and shear stability models. In the first case, chip separation is reported to occur when the plastic shear strains reach a fracture limit. On the other hand, shear stress models assume the fracture onset is governed by a critical value of shear stress. For some materials and cutting conditions, formation of a discontinuous chip is explained by shear instability models, which usually assume that localized plastic deformation associated with thermal softening causes the material to fracture according to a defined pattern [1].

Several studies on numerical simulation of sheet blanking process have been reported. Brokken [5] proposed an Euler-Lagrangian method combined with re-meshing techniques. Morancay [6] used a failed elemenet deactivation procedure for simulating this class of problems. Rachik [7] used Arbitrary Lagrangian Eulerian (ALE) method for re-meshing process. In all cases, a predefined deformable mesh is expected to experience large distortions, accompanied by very noticeable errors. This suggests the use of re-meshing techniques in order to reduce the overall error and provide a reliable solution.

Adaptive Re-meshing

The key to the efficient and economic solution of problems is not merely the number of nodes and elements but also their placement. Regions with large gradients (e.g., a discontinuity or stress concentration) will need a high mesh density, with quiescent regions requiring a comparatively coarser mesh. The ideal is that every element contains the same predefined, allowable error, thus yielding an optimal mesh. In general, adaptive re-meshing techniques encompass two main aspects: error estimation and transfer operations:

Error estimation

Error estimation has gained considerable momentum when Zienkiewicz and Zhu [8] introduced error estimates based on post-processing techniques of the finite element solutions which could easily be used in conjunction with mesh refinement strategies.

The theory of continuous damage mechanics postulates the elasto-plastic degradation of the material, which is quantified by the damage variable, D, and is governed by a damage law. In this paper, Lemaitre's [9] isotropic damage model has been adopted, in which D is the local ratio between the areas of micro-voids and the total areas of the material and ranges from 0 (virgin material) to 1 (rupture). The damage strain release rate parameter, $-Y$, is defined by

$$-Y(T_H, J_2) = \frac{J_2(T)^2}{2E(1-D)^2}\left[\frac{2}{3}(1+\nu) + 3(1-2\upsilon)\left(\frac{\sigma_H}{J_2(T)}\right)^2\right] \tag{1}$$

Where σ_H and J_2 are the hydrostatic stress and Von Mises equivalent stress respectively and T is the rotated stress tensor. The rate of the damage work, ω_D, is

$$\omega_D = (-Y)\dot{D} \tag{2}$$

The approximation error for a generic element K and its corresponding global value are

$$\varepsilon^2_{\omega_D} = \sum_K \varepsilon^2_{\omega_D,K} \quad , \quad \varepsilon^2_{\omega_D,K} := \int_K [(-Y)^* - (-Y)^h](\dot{D}^* - \dot{D}^h)\, d\Omega \tag{3}$$

The ideal mesh requires as equal distribution of element errors, $\eta_{\omega_D,K}$, which have been defined as

$$\eta_{\omega_D,K} = \frac{\varepsilon_{\omega_D,K}}{\left(\dfrac{\omega^h{}_D + \varepsilon_{\omega_D}{}^2}{m}\right)^{1/2}} \tag{4}$$

where m is the number of elements and ω_D and $\omega^h{}_D$ are given respectively by

$$\omega_D = \sum_K (-Y):\dot{D} \quad , \quad \omega^h{}_D = \sum_K (-Y)^h : \dot{D}^h \tag{5}$$

Therefore, the target error, η_K, and current error, $\eta_{\omega_D,K}$, define the error index, ξ_K, as

$$\xi^{\omega_D}{}_K = \frac{\eta_{\omega_D,K}}{\eta_K} = \frac{\varepsilon_{\omega_D,K}}{\eta_K\left(\dfrac{\omega^h{}_D + \varepsilon_{\omega_D}{}^2}{m}\right)^{1/2}} \tag{6}$$

The new element size h is computed by (p is the degree of the interpolation polynomial**)**

$$h_{new,K} = \frac{h_{old,K}}{(\xi^{\omega_D}{}_K)^{1/p}} \tag{7}$$

Transfer Techniques

In elastic-plastic problems, there exist two basic types of variables to be transferred, i.e., nodal values such as displacements and velocity, and quantities associated to the quadrature points such as internal energy density, the equivalent plastic strain, plastic strain tensor. Here, the methodology proposed by Peric[10] and Dutko [11] is adopted, where two separate but compatible transfer operators, namely τ_1 and τ_2 for Gauss point and nodal variables, respectively, are defined.

For simplicity of notation, the state array $\Lambda(h,n) = \widetilde{\Lambda}(h,n) \bigcup \hat{\Lambda}(h,n)$ is defined, which contains all nodal, $\hat{\Lambda}(h,n)$, and Gauss point, $\widetilde{\Lambda}(h,n)$, information at a given time step t_n and mesh h. When the estimated error of the solution $\Lambda(h,n)$ violates a prescribed criterion at time t, a new mesh, h+1, is generated and a new solution $\Lambda(h+1, n+1)$ is computed.

The transfer operator τ_1

The process comprises three distinct steps, i.e., projection of the Gauss point variables to nodes, transfer of the nodal values from the old to the new mesh and projection of the corresponding nodal quantities to new quadrature points.

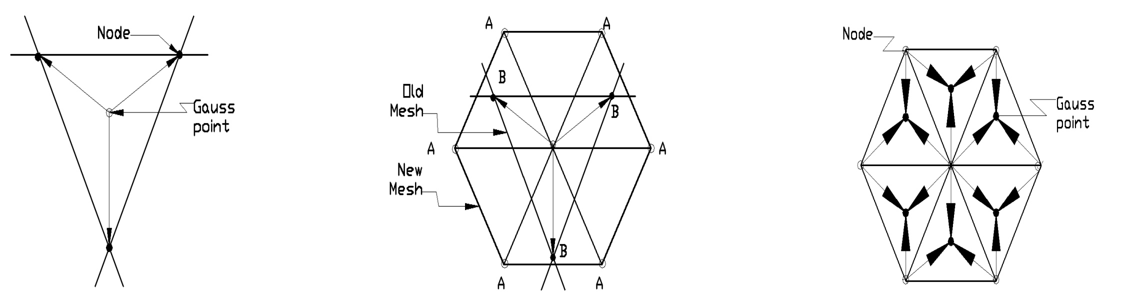

a) Projection of variables to nodes b) Transfer from old to new mesh c) Nodes to Gauss point interpolation

Figure 1– Transferring Gauss point variables from old to the new mesh.

(a) Projecting Gauss point variables to nodes

The transfer of Gauss point variables to nodes is performed using the well-known projection/smoothing technique, largely used for error estimates and based on Zienkiewicz and Zhu's [12] approach. Fig. 1(a) illustrates the operation for constant strain triangles, where the subscripts N and G indicate nodal and Gauss point variables, respectively.

(b) Transferring the nodal projection to the new mesh

The second step (Fig. 1(b)) is the most complex, in which the projection/smoothed components of the state array, $\widetilde{\Lambda}^*(h,n,N)$, are transferred from old mesh h to the new mesh h+1. The process can be subdivided into three stages. In the first stage, for every node A of the new mesh h+1 with coordinates ${}^{h+1}x_{n,A}$, a background element, ${}^{h}\Omega^e$, is found in the old mesh for which ${}^{h+1}x_{n,A} \in {}^{h}\Omega^e$.

The second stage constitutes the evaluation of the local coordinates, $({}^h\xi_A, {}^h\eta_A)$, of the node A of the new mesh within the background element by solving

$$ {}^{h+1}x_{n,A} = \sum_{b=1}^{r} {}^hN_b({}^h\xi_A, {}^h\eta_A)\ {}^hx_{n,b} \tag{8} $$

where r is the number of nodes of element and N is the interpolation function. In the third stage, the state variables $\widetilde{\Lambda}(h+1,n,N)$ are mapped from nodes B of the old mesh to nodes A of the new mesh h+1 by using the interpolation function ${}^hN_b({}^h\xi_A, {}^h\eta_A)$ as

$$ \widetilde{\Lambda}(h+1,n,A) = \sum_{b=1}^{r} {}^hN_b({}^h\xi_A, {}^h\eta_A)\,\widetilde{\Lambda}^*(h,n,b) \tag{9} $$

(c) Interpolating Gauss point variable in the new mesh

In the final step, which is illustrated in Fig. 1(c), Gauss point variables $\widetilde{\Lambda}(h+1,n,G)$ of the new mesh are obtained by using the interpolation function of the element ${}^{h+1}\Omega^{(e)}$ as

$$ \widetilde{\Lambda}(h+1,n,G) = \sum_{a=1}^{r} {}^{h+1}N_a({}^{h+1}\xi_G, {}^{h+1}\eta_G)\,\widetilde{\Lambda}\,(h+1,n,a) \tag{10} $$

in which $({}^{h+1}\xi_G, {}^{h+1}\eta_G)$ are the Gauss point coordinates.

The transfer operator τ_2

The present task reproduces the mapping of the nodal values operation as

$$ \hat{\Lambda}(h+1,n,A) = \sum_{b=1}^{r} {}^hN_b({}^h\xi_A, {}^h\eta_A)\,\hat{\Lambda}(h,n,b) \tag{11} $$

Numerical Simulation

Chip Separation

In order to simulate the discontinuous chip separation; in which the cutting plane should not be predefined, Owen [2] used a failure criterion based on the Lemaitre's damage model [12] for this class of problems as

$$ I_D = \int_0^{\varepsilon_p} \left\{ \frac{\sigma^2_Y}{2E} \left[\frac{2}{3}(1+\upsilon) + 3(1-2\upsilon)\left(\frac{\sigma_H}{\sigma_Y}\right)^2 \right] \right\} d\varepsilon_p \tag{12} $$

This criterion has shown good agreement with the experimental results [2] and has been adopted in this work. In this criterion any node which reaches to a critical value, would be separated, therefore, to avoid spurious fractures, the criterion should be able to predict the fracture zone and to exhibit a high gradient near the critical zone. These requirements have already been in the failure criteria introduced by Komanduri [13], using experimental techniques based on scanning electron microscopy and a high-speed movie camera, proposed a chip formation model for titanium alloys (Ti-6Al-4V). In this paper the same material data have been adopted from the Komanduri's experimental work. The experimental results, initial mesh, material properties and problem specification are depicted in Fig 2.

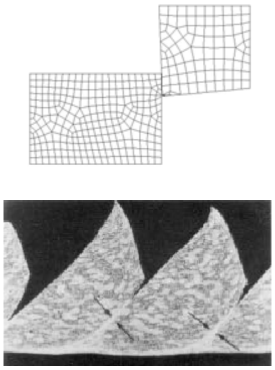

Rake angle	-3 deg
Flank angle	5 deg
Cutting speed	10 m/s
Cutting depth	0.5mm
Initial temperature	298 K
Initial yield stress	1231.5 MPa
Initial plastic strain	0.008

Young's modulus	115.7 GPa
Poisson's ratio	0.321
Specific mass	4420 Kg/m³
Thermal conductivity	586.2 J/Kg.K
Hardening parameter	0.059
Specific heat	582.2 J/Kg.K
Coulomb friction	0.1

Figure 2- Initial mesh, experimental results, material properties and problem specification

The yield stress adopted in the simulations is given as an input to the program by the equation

$$\sigma_y = \sigma_{y\circ}(E_p + E_{p\circ})^n - 2.3e6(T - T_\circ) \qquad (13)$$

Fig. 3 shows the procedure of adaptive re-meshing in different time steps, corresponding to the deformation of tool, Δu, for three different tool advances Δu = 0.156, 0.258 and 0.536 mm. In this figure, formation of two shear bands is clearly observed at the final stage of the process. Fig. 4 illustrates the distribution of plastic strain. According to figures 3 and 4, two regions with higher mesh density distribution during the re-meshing procedure are observed. The first region is the area between the tool and work piece in which a high contact stress exists and so finer elements are generated. The second region belongs to high value of plastic strain (strain localization) region, where shear band is expected to occur.

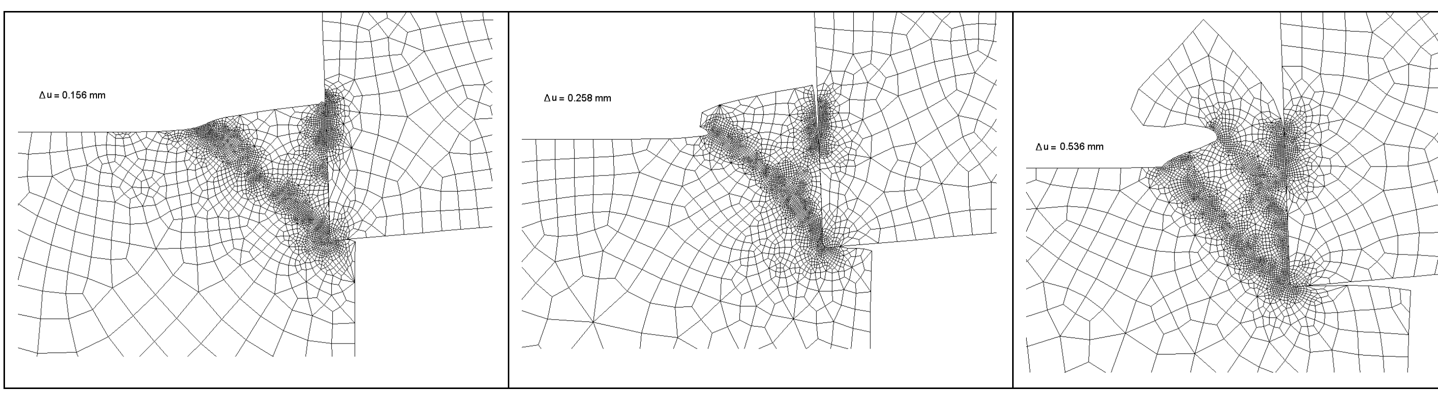

Figure 3 - Adaptive re-meshing and chip separation

A good agreement with experiental data by Komanduri [13] which reported formation of shear bands at angles near to 45 degrees is observed. The same problem has been simulated by Owen [2, 3] (Fig. 5). It is clearly found that more realistic formation of chip separation; especially the first chip, tool advance and formation of the shear-band are achieved by the present work.

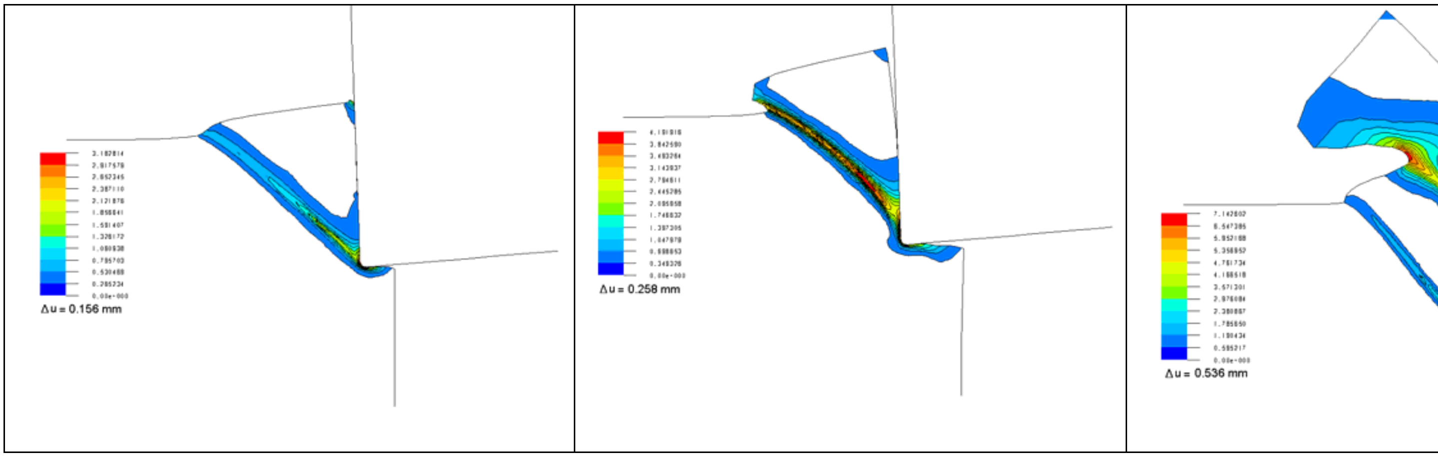

Figure 4 – Distribution of plastic strain

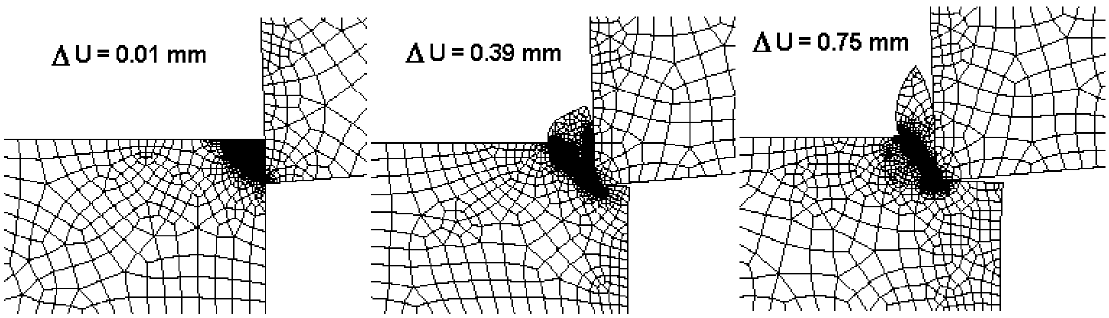

Figure 5 – Adaptive re-meshing reported by Owen and Vaz Jr [3]

Blanking

The same algorithm for chip separation has been used to simulate another metal cutting process called blanking. The geometry of problem and problem specifications are depicted in Fig. 6. The punch moves downwards at 10 m/s while the die and upper support hold the metal sheet.

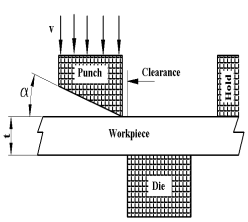

Shear angle	0 deg
Thickness	3 mm
Punch speed	10 m/s
Clearance	0.09 mm
Initial temperature	298 K
Initial yield stress	1231.5 MPa
Initial plastic strain	0.008

Young's modulus	115.7 GPa
Poisson's ratio	0.321
Specific mass	4420 Kg/m³
Thermal conductivity	586.2 J/Kg.K
Hardening parameter	0.059
Specific heat	582.2 J/Kg.K
Coulomb friction	0.1

Figure 6- Material properties and problem specification

The distribution of mesh density by using adaptive re-meshing in blanking process is presented for different punch displacement (Δu) in Figure 7. At the beginning of the procedure (Δu=0.024 mm) two regions have more density of mesh than other regions, where the first region is the interface of punch with the work piece; the place of high contact stress, and the second is the region that work piece is forced by the corner of the lower die, which creates a very high stress concentration due to the sharp corner.

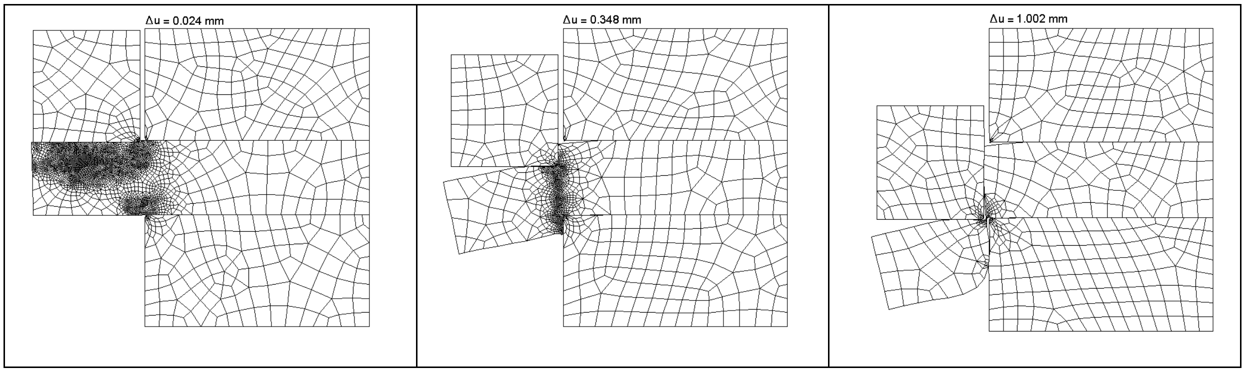

Figure 7- Adaptive re-mesh in blanking process

At Δu=0.348 mm the high mesh density region is generated along the cutting plane across the thickness of work piece. At this load step because of the deformation of the work piece, the contact area between work piece and punch is less than previous load step (Δu=0.024 mm), so mesh refinement occurs only in that small part. By following the procedure, it is found that at the end of the process no high-density mesh is generated and a rather uniform distribution of coarse mesh is required for discretization of the model, and no major element distortion exists within the model. The distribution of plastic strain in this process is presented in Figure 8.

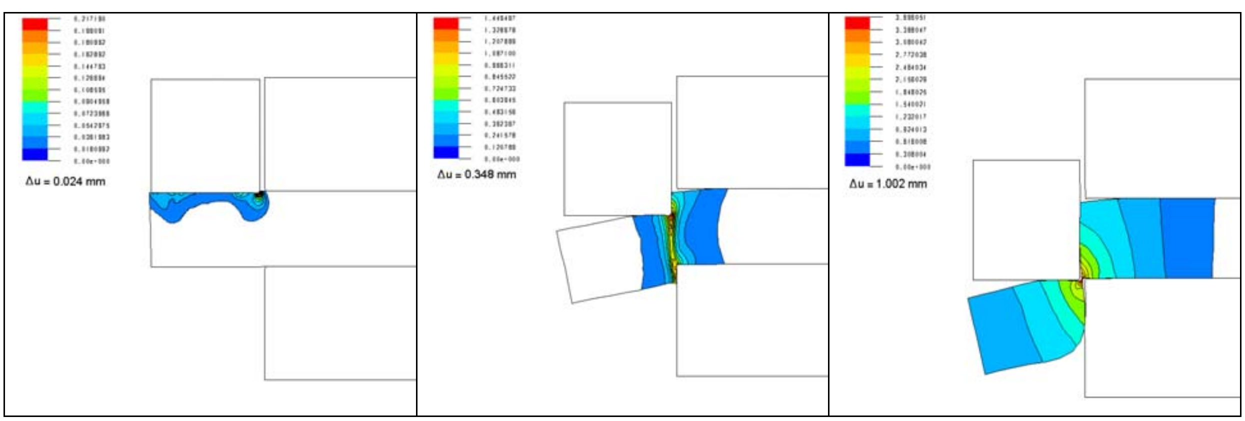

Figure 8 – Distribution of plastic strain

Conclusion

Element distortion is a major factor in machining and cutting simulation, thereby requiring periodical re-meshing. Within the present work, error indicators based on the rate of damage work has been proposed for damage of materials. The assessment of the estimator is based on several metal cutting tests and shows that this indicator is able to capture shear band formation efficiently. The successful application of the error estimator based on the integration of Lemaitre's damage model to orthogonal machining and blanking, confirms the good performance as previously reported.

References

1- J. Q. Xie, A. E. Boyoumi, H. M. Zbib, Analytical and experimental study of shear localization in chip formation in orthogonal machining, J. Materials Engng. Perf. 4 (1995) 32-39.

2- D.R.J. Owen M. Vaz Jr.,Computational techniques applied to high-speed machining under adiabatic strain localization conditions, Comp. Meth. Appl. Mech. Eng. 171 (1999) 445-461.

3- M. Vaz Jr., Computational Approaches to Simulation of Metal Cutting Problems, PhD thesis, Department of Civil Engineering, University of Wales Swansea, Swansea,UK, 1998.

4- S. Kalpakjian, Manufacturing processes for engineering materials, (Addison Wesley, 1984).

5- D. Brokken, A. M. Goijaerts, W. A. M. Brekelmans, C. W J. Oomens, Modeling of the blanking process, In D. R. J. Owen, E. Onate, and E. Hinton. Editors, Computational Plasticity: Theory and Application, Vol. 2 (Barcelona, CIMNE, 1997) 1417-1424.

6- L. Morancay, M. Homsi, J. M. Roelandz, Application of re-meshing technics to the simulation of metal cutting by punching, In D. R. J. Owen, E. Onate, and E. Hinton. Editors, Computational Plasticity (1997) 611-618.

7- M. Rachik, J. M. Roelendt, A. Maillard, A unified approach for metal blanking numerical simulation, European Congress on Computational Methods in Applied Siences and Engineering (ECCOMAS, Barcelona, 2000).

8- O. C. Zienkiewicz, J. Z. Zhu, A simple error estimator and adaptive procedure for practical engineering analysis, Int. J. Num. Meth. Eng. 24 (1987) 337-357.

9- J. Lemaitre, How to use damage mechanics, Nuclear. Engng. Design 80 (1984) 233-245.

10- D. Peric, C. Hochard, M. Dutko, D. R. J. Owen, Transfer operators for evolving meshes in small strain elasto-plasticty, Comp. Mech. Appl. Mech. Eng. 137 (1996) 331-344.

11- M. Dutko, D. Peric, D. R. J. Owen, Z. Wei, J. Yu, Bulk forming simulation by adaptive explicit FEM, Computational Plasticity: Theory and Applications 2 (Barcelona, CIMNE, 1997) 1305-1312.

12- J. Lemaître, A continuous damage mechanics model for ductile fracture, J. Engng. Mat. Tech., Trans. ASME 107 (1985) 83-89.

13- R. Komanduri, T. Schroeder, J. Hazra, B. F. Von Turkovich, D. G. Flom, On the catastrophic shear instability in high-speed machining of an AISI 4340 steel, J. Engng. Ind., Trnas. ASME 104 (1982) 121-131.